J|A|C|S ARTICLES

Published on Web 12/30/2009

Tailored Synthetic Polyamines for Controlled Biomimetic Silica Formation

Anja Bernecker,[†] Ralph Wieneke,[‡] Radostan Riedel,[‡] Michael Seibt,[§] Armin Geyer,*[,‡] and Claudia Steinem*[,†]

Institute of Organic and Biomolecular Chemistry, University of Göttingen, Tammannstr. 2, 37077 Göttingen, Germany, Philipps-Universität Marburg, Hans-Meerwein-Strasse, 35032 Marburg, Germany, and IV. Physikalisches Institut, University of Göttingen, Friedrich-Hund-Platz 1, 37077 Göttingen, Germany

Received July 22, 2009; E-mail: geyer@staff.uni-marburg.de; claudia.steinem@chemie.uni-goettingen.de

Abstract: Organic compounds isolated from diatoms contain long-chain polyamines with a propylamine backbone and variable methylation levels and chain lengths. These long-chain polyamines are thought to be one of the important classes of molecules that are responsible for the formation of the hierarchically structured silica-based cell walls of diatoms. Here we describe a synthetic route based on solid-phase peptide synthesis from which well-defined long-chain polyamines with different chain lengths, methylation patterns, and subunits can be obtained. Quantitative silica precipitation experiments together with structural information about the precipitated silica structures gained by scanning and transmission electron microscopy revealed a distinct dependence of the amount, size, and form of the silica precipitates on the molecular structure of the polyamine. Moreover, the influence of the phosphate concentration was elucidated, revealing the importance of divalent anions for the precipitation procedure. We were able to derive further insights into the precipitation properties of long-chain polyamines as functions of their hydrophobicity, protonation state, and phosphate concentration, which may pave the way for better control of the formation of nanostructured silica under ambient conditions.

Introduction

Silica is one of the most abundantly used materials in the world. The chemical synthesis of silica-based materials such as molecular sieves, resins, and catalysts relies on extreme conditions of temperature, pressure, and pH. Under these conditions, control of complex three-dimensional structures on the nanometer to micrometer scale remains tedious. However, for example, nanometer-sized mesoporous silica particles have attracted much interest in nanotechnology in recent years because they have many attractive features, such as high pore volume, large surface area, and ease of functionalization.[1] The highly porous materials can be utilized in the storage and delivery of small molecules and thus can be used in catalysis, drug delivery, and imaging.

In comparison with these processes, control of the formation of hierarchically ordered, well-defined three-dimensional silica structures under mild synthetic conditions is very well realized in organisms such as sponges, diatoms, and radiolaria.[2−4] Diatoms, ubiquitous unicellular photosynthetic organisms in the marine ecosystem, are very well known for the spectacular design of their silica-based cell walls.[5] Hence, considerable research has been directed toward identifying the mechanisms involved in the biosilification process that results in hierarchically ordered siliceous diatom shells (frustules) in order to understand this procedure and as a result to control and tailor silica formation. Using mild conditions for silification might offer the possibility of protecting sensitive molecules and creating biochemical sensors, as proteins[6] and even cells[7] are not harmed by encapsulation. Two main types of organic compounds are intimately associated with the diatom shell. One of these types consists of (poly)peptides with propylamino-functionalized lysine side chains and phosphorylated serine side chains, which are called silaffins.[8−11] The other major group is a series of long-chain polyamines[12−14] that have also recently

[†] Institute of Organic and Biomolecular Chemistry, University of Göttingen.

[‡] Philipps-Universität Marburg.

[§] IV. Physikalisches Institut, University of Göttingen.

(1) Liong, M.; Angelos, S.; Choi, E.; Patel, K.; Stoddart, J. F.; Zink, J. I. *J. Mater. Chem.* **2009**, *19*, 6251–6257.
(2) Hildebrand, M. *Chem. Rev.* **2008**, *108*, 4855–4874.
(3) Schröder, H. C.; Wang, X.; Tremel, W.; Ushijima, H.; Muller, W. E. *Nat. Prod. Rep.* **2008**, *25*, 455–474.
(4) Brutchey, R. L.; Morse, D. E. *Chem. Rev.* **2008**, *108*, 4915–4934.
(5) Round, F. E.; Crawford, R. M.; Mann, D. G. *The Diatoms*; Cambridge University Press: Cambridge, U.K., 1990.
(6) Dickerson, M. B.; Sandhage, K. H.; Naik, R. R. *Chem. Rev.* **2008**, *108*, 4935–4978.
(7) Yang, S. H.; Lee, K. B.; Kong, B.; Kim, J. H.; Kim, H. S.; Choi, I. S. *Angew. Chem., Int. Ed.* **2009**, *48*, 9160–9163.
(8) Kröger, N.; Deutzmann, R.; Sumper, M. *Science* **1999**, *286*, 1129–1132.
(9) Kröger, N.; Deutzmann, R.; Sumper, M. *J. Biol. Chem.* **2001**, *276*, 26066–26070.
(10) Poulsen, N.; Sumper, M.; Kröger, N. *Proc. Natl. Acad. Sci. U.S.A.* **2003**, *100*, 12075–12080.
(11) Wenzl, S.; Deutzmann, R.; Hett, R.; Hochmuth, E.; Sumper, M. *Angew. Chem., Int. Ed.* **2004**, *43*, 5933–5936.
(12) Kröger, N.; Deutzmann, R.; Bergsdorf, C.; Sumper, M. *Proc. Natl. Acad. Sci. U.S.A.* **2000**, *97*, 14133–14138.
(13) Kröger, N.; Poulsen, N. *Annu. Rev. Genet.* **2008**, *42*, 83–107.

been found in marine sponges.[15] These polyamines have been characterized as poly(propyleneimine) chains with up to 20 repeat units, attached to putrescine or 1,3-diaminopropane.[12,15,16] The complex mixture of long-chain polyamines that diatoms synthesize appears to be composed in a species-specific manner, suggesting its important function in structure formation of the silica shell. In vitro, these polyamines have been shown to rapidly precipitate silica spheres with diameters of several hundreds of nanometers.[12,17] Sumper[18] proposed a templating mechanism based on a phase separation model that explains the hierarchy of hexagonal silica structures producing the highly symmetric valve patterning. The basic principle is the formation of polyamine-containing droplets that consecutively segregate into smaller droplets upon silica precipitation at the surface of the droplet. Species-specific patterns result from variations in the polyamine droplet size established during the very first phase separation process.[16] This, in turn, defines the wall-to-wall distance of the largest hexagonal framework. Control of the polyamine droplet size during phase separation is the crucial point of the model. Sumper and Brunner[16] have suggested that divalent anions such as phosphate play a major role in determining the size of these nanodroplets.

In previous work, long-chain polyamines synthesized by polymerization, leading to molecules with distributed chain lengths,[19−21] or short alkylamines such as spermine, spermidine, and their analogues[22−24] as well as tripropylenetetramine and pentapropylenetetramine[25] have been investigated in terms of their precipitation capability. They induce rapid precipitation of silica spheres from silicic acid solutions on a short time scale. However, well-defined long-chain polyamines with more than seven amino group-containing units have not yet been synthesized and investigated.

Here we provide a general strategy for synthesizing well-defined long-chain polyamines with a number of nitrogen atoms similar to that found in polyamines of diatoms. The silica-precipitating properties of such polyamines were investigated, with particular emphasis on their molecular structure and the influence of phosphate anions. From the obtained results, we expect to gain new insights into in vitro silica formation that may pave the way for control of nanostructured silica.

Results

Synthetic Strategy. To date, only long-chain polyamines synthesized by polymerization, leading to molecules of distributed chain lengths,[19−21] have been investigated in terms of their precipitation capabilities. In this work, we have developed a strategy based on solid-phase peptide synthesis (SPPS) that enables the generation of well-defined long-chain polyamines with more than seven amino group-containing units. The strategy is outlined in Scheme 1. SPPS with temporary Fmoc protection on a trityl resin yielded the resin-bound oligoamide precursors. Reduction of oligoamides with borane at elevated temperatures is the most popular method for the synthesis of secondary amines in solution,[26−28] and Hall and co-workers[29−31] as well as Houghten and co-workers[32−35] have described reductions on solid supports. A disadvantage of the method, however, is the formation of relatively stable aminoborane complexes under the reaction conditions, which require special workup.[31,36] Most of the published protocols are not compatible with the trityl resin.[35] Thus, an adaption of basic conditions for the release of the

Scheme 1. General Procedure for the Solid-Phase Synthesis of Long-Chain Polyamines

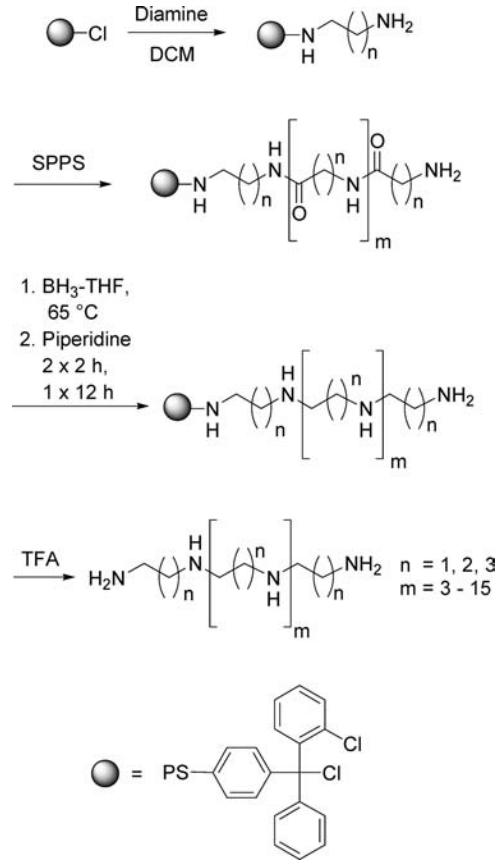

(14) Sumper, M.; Brunner, E.; Lehmann, G. *FEBS Lett.* **2005**, *579*, 3765–3769.
(15) Matsunaga, S.; Sakai, R.; Jimbo, M.; Kamiya, H. *ChemBioChem* **2007**, *8*, 1729–1735.
(16) Sumper, M.; Brunner, E. *Adv. Funct. Mater.* **2006**, *16*, 17–26.
(17) Sumper, M.; Lorenz, S.; Brunner, E. *Angew. Chem., Int. Ed.* **2003**, *42*, 5192–5195.
(18) Sumper, M. *Science* **2002**, *295*, 2430–2433.
(19) Brunner, E.; Lutz, K.; Sumper, M. *Phys. Chem. Chem. Phys.* **2004**, *6*, 854–857.
(20) Patwardhan, S. V.; Mukherjee, N.; Steinitz-Kannan, M.; Clarson, S. J. *Chem. Commun.* **2003**, 1122–1123.
(21) Behrens, P.; Jahns, M.; Menzel, H. In *Handbook of Biomineralization*; Behrens, P., Bäuerlein, E., Eds.; Wiley-VCH: Weinheim, Germany, 2007; Vol. 2, pp 3−18.
(22) Belton, D. J.; Patwardhan, S. V.; Perry, C. C. *J. Mater. Chem.* **2005**, *15*, 4629–4638.
(23) Belton, D. J.; Patwardhan, S. V.; Annenkov, V. V.; Danilovtseva, E. N.; Perry, C. C. *Proc. Natl. Acad. Sci. U.S.A.* **2008**, *105*, 5963–5968.
(24) Annenkov, V. V.; Patwardhan, S. V.; Belton, D.; Danilovtseva, E. N.; Perry, C. C. *Chem. Commun.* **2006**, 1521–1523.
(25) Noll, F.; Sumper, M.; Hampp, N. *Nano Lett.* **2002**, *2*, 91–95.
(26) Brown, H. C.; Heim, P. *J. Org. Chem.* **1973**, *38*, 912–916.
(27) Brown, H. C.; Narasimhan, S.; Choi, Y. M. *Synthesis* **1981**, 441–442.
(28) Roeske, R. W.; Weitl, F. L.; Prasad, K. U.; Thompson, R. M. *J. Org. Chem.* **1976**, *41*, 1260–1261.
(29) Hall, D. G.; Laplante, C.; Manku, S.; Nagendran, J. *J. Org. Chem.* **1999**, *64*, 698–699.
(30) Wang, F.; Manku, S.; Hall, D. G. *Org. Lett.* **2000**, *2*, 1581–1583.
(31) Manku, S.; Laplante, C.; Kopac, D.; Chan, T.; Hall, D. G. *J. Org. Chem.* **2001**, *66*, 874–885.
(32) Nefzi, A.; Giulianotti, M. A.; Ong, N. A.; Houghten, R. A. *Org. Lett.* **2000**, *2*, 3349–3350.
(33) Nefzi, A.; Ostresh, J. M.; Giulianotti, M.; Houghten, R. A. *J. Comb. Chem.* **1999**, *1*, 195–198.
(34) Nefzi, A.; Ostresh, J. M.; Houghten, R. A. *Tetrahedron* **1999**, *55*, 335–344.
(35) Nefzi, A.; Ostresh, J. M.; Meyer, J.-P.; Houghten, R. A. *Tetrahedron Lett.* **1997**, *38*, 931–934.
(36) Lane, C. F. *Aldrichimica Acta* **1973**, *6*, 51–58.

Table 1. Molecular Structures of the Polyamines under Investigation and Corresponding Mass Spectrometric Analysis Data and Yields

Name	Formula	Structure	Calcd. for	Found for	Yield
C2N7	$C_{12}H_{33}N_7$	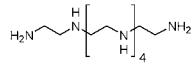	$[M+Na]^+$ 298.3	$[M+Na]^+$ 298.3 [a]	176 mg (0.16 mmol; 34 %)
C3N7	$C_{18}H_{45}N_7$	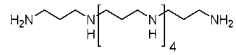	$[M+H]^+$ 360.4	$[M+H]^+$ 360.4 [a]	54 mg (50 μmol; 72 %)
C4N7	$C_{24}H_{57}N_7$	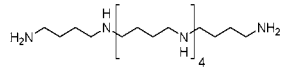	$[M+H]^+$ 444.4	$[M+H]^+$ 444.4 [a]	380 mg (0.31 mmol; 64 %)
C3N6	$C_{15}H_{38}N_6$	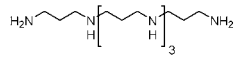	$[M+H]^+$ 303.32	$[M+H]^+$ 303.32 [b]	135 mg (140 μmol; 85 %)
C3N12	$C_{33}H_{80}N_{12}$	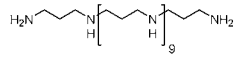	$[M+H]^+$ 645.7	$[M+H]^+$ 645.7 [a]	149 mg (90 μmol; 61 %)
C3N18	$C_{51}H_{122}N_{18}$	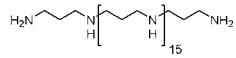	$[M+H]^+$ 988.0	$[M+H]^+$ 988.2 [a]	137 mg (51 μmol; 56 %)
C3N12Me	$C_{43}H_{70}N_{12}$	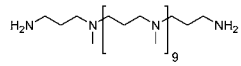	$[M+H]^+$ 785.8	$[M+H]^+$ 785.8 [a]	25 mg (21 μmol; 31 %)

[a] Obtained using matrix-assisted laser desorption ionization (MALDI) mass spectrometry. [b] Obtained using electrospray ionization (ESI) mass spectrometry.

secondary amines was needed in our case.[37,38] The best results were obtained after repeated washing with piperidine, as described in the experimental section in the Supporting Information.

The synthesis of C3N12Me (Table 1) required a methylation step before the oligoamide synthesis, as outlined in Scheme 2. Aliquots of the polyamide precursors were cleaved from the resin during SPPS and analyzed by mass spectrometry and spectroscopic methods. All of the analytical data were in full agreement with the supposed structures. The compounds together with their yields and mass spectrometric characterization data are summarized in Table 1.

Variation of the N-to-N Distance in Polyamines. The major components of the polyamines found in diatoms are composed of propyleneimine units. We wondered whether the distance between two adjacent amino groups, the catalytically active sites of silica formation, is a decisive parameter for SiO_2 precipitation. Thus, we performed precipitation experiments in the presence of three different synthetic polyamines, termed C2N7, C3N7, and C4N7 (Table 1). All three of these polyamines contain the same number of nitrogen atoms but vary in the number of C atoms between the amino groups. The amount of precipitated silica, as determined by the β-silicomolybdate method,[39] varied considerably with the N-to-N distance. While for C2N7 only a very small amount of precipitation was found, with a silicon mass (m_{Si}) of 1.4 ± 0.6 μg ($n = 7$), m_{Si} increased significantly, by almost a factor of 8, to 10.6 ± 3.7 μg ($n = 8$) for C3N7. An even longer spacer of four C atoms, C4N7, only doubled the mass in comparison with C3N7, affording $m_{Si} = 21.6 \pm 2.2$ μg ($n = 8$). The fact that C2N7 precipitated only a very small amount of SiO_2 is also reflected in the scanning electron microscopy (SEM) images showing sparse aggregates of small silica spheres with an average diameter of $d_{C2N7} = 38 \pm 15$ nm

Scheme 2. Solid-Phase Synthesis of C3N12Me

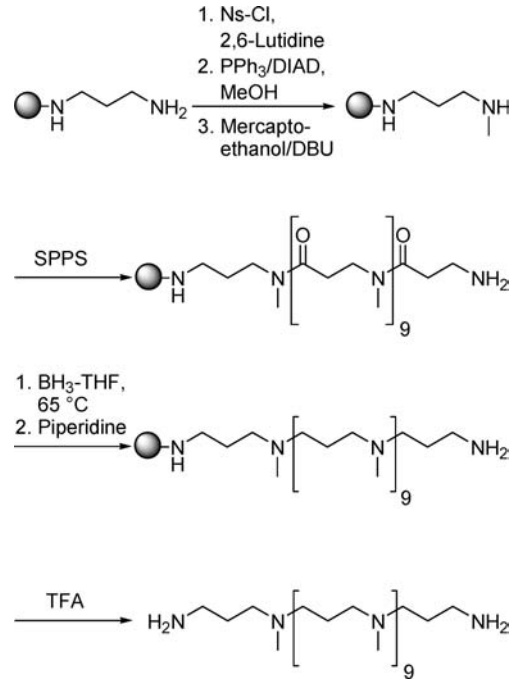

(37) Baldwin, R.; Washburn, R. *J. Org. Chem.* **1961**, *26*, 3549–3550.
(38) Young, D. E.; McAchran, G. E.; Shore, S. G. *J. Am. Chem. Soc.* **1966**, *88*, 4390–4396.
(39) Iler, R. K. *The Chemistry of Silica*; Wiley: New York, 1979.

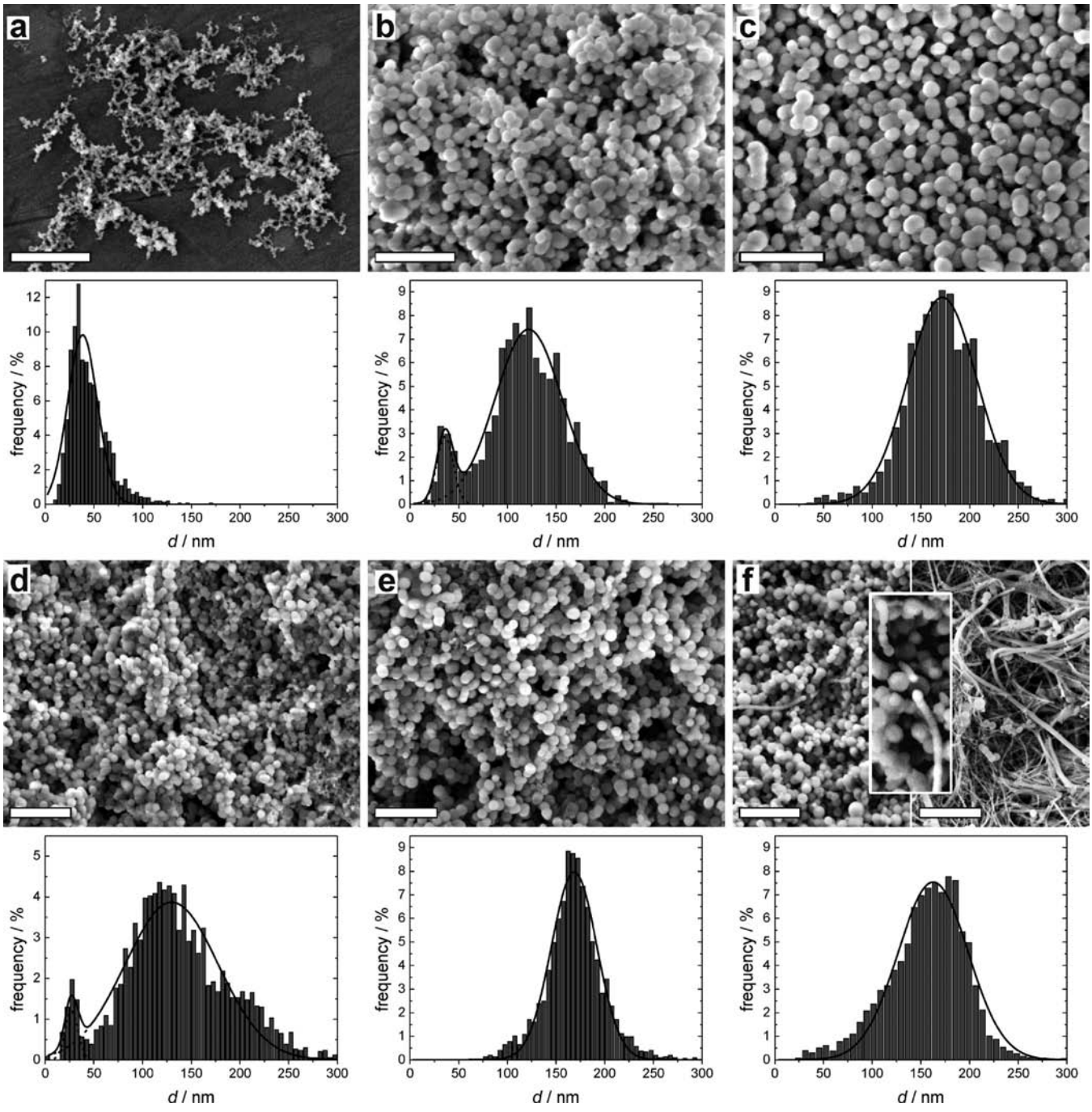

Figure 1. (top) SEM images and (bottom) histogram analyses of the silica structures of the precipitates formed in the presence of (a) C2N7, (b) C3N7, (c) C4N7, (d) C3N6, (e) C3N12, and (f) C3N18. All of the precipitates were obtained in 30 mM phosphate buffer (pH 6.8) with $c_N = 1$ mM and $c_{Si(OH)_4} = 100$ mM. The reaction time was 10 min. Scale bars are 1 μm.

(Figure 1a). Spheres were also found for C3N7- and C4N7-induced precipitates (Figure 1b,c). However, in case of C3N7, two different populations of silica spheres could be distinguished. A small fraction of the spheres had the same diameter ($d_{1\text{-C3N7}} = 36 \pm 8$ nm) as those formed in the presence of C2N7, while the majority of the spheres were significantly larger ($d_{2\text{-C3N7}} = 122 \pm 34$ nm). Even larger were the silica spheres precipitated in the presence of the polyamine C4N7, with $d_{C4N7} = 172 \pm 35$ nm. From these results, it becomes obvious that the distance between the amino groups significantly alters not only the amount of precipitated silica but also the size of the silica spheres.

Chain Lengths of the Polyamines. In all diatoms, polyamines with rather long chains of 7−18 amino groups are found. Here we investigated how the chain length of the polyamine influences the amount and structure of the silica precipitate. Three different polyamines were investigated. In accordance with the propyl spacer found in natural polyamines and the results obtained in the previous section, all of the compounds were composed of propyleneimine units, the shortest having four (C3N6), the intermediate 10 (C3N12), and the longest 16 units (C3N18) (Table 1). As the amino groups are the catalytically active sites for precipitation, the number of nitrogen atoms was chosen to be identical in each sample ($c_N = 1$ mM). The amount

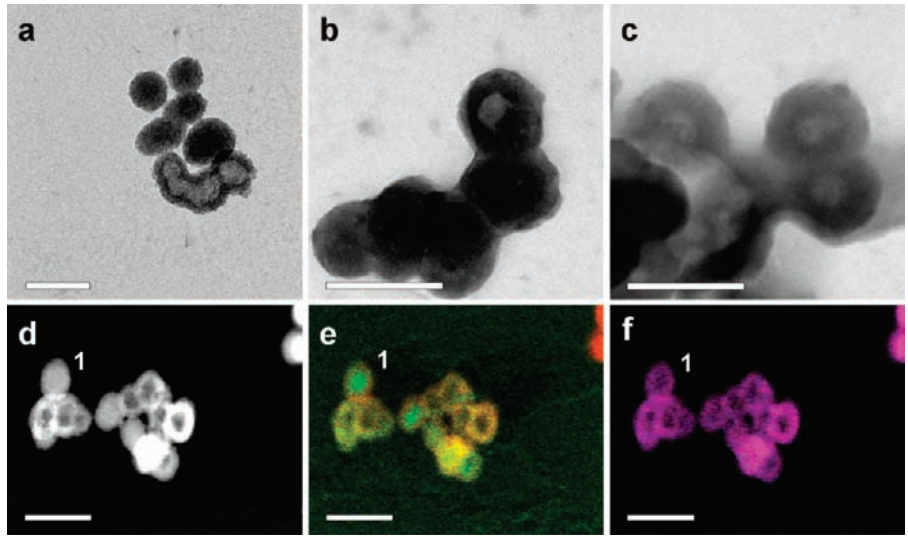

Figure 2. (a−c) Characteristic TEM bright-field micrographs of a silica precipitate induced by C3N6. (d) STEM annular dark-field micrograph of a silica precipitate. (e, f) EDX element maps showing overlays of (e) the silicon (red) and carbon (green) signals and (f) the silicon (red) and oxygen (blue) signals. The precipitates were obtained in 30 mM phosphate buffer (pH 6.8) with $c_N = 1$ mM and $c_{Si(OH)_4} = 100$ mM. The reaction was stopped after 10 min. Scale bars are 200 nm.

of precipitated silica was found to be a linear function of the number of propyleneimine units. While for C3N6 an amount of 9.0 ± 2.6 μg ($n = 32$) of silicon was found, C3N12 precipitated $m_{Si} = 14.0 \pm 1.5$ μg ($n = 20$). For C3N18, m_{Si} was determined to be 22.0 ± 1.7 μg ($n = 32$). For C3N6, SEM images demonstrated that silica spheres with a rather broad size distribution ($d_{2\text{-C3N6}} = 130 \pm 48$ nm) were formed (Figure 1d). A minor fraction of small spheres with $d_{1\text{-C3N6}} = 27 \pm 5$ nm was also visualized by means of SEM. In the case of C3N12-induced silica precipitates, a single much more narrow distribution of silica spheres was found, with an average diameter of $d_{C3N12} = 169 \pm 23$ nm (Figure 1e). The morphology of the silica structures changed considerably when C3N18 was used. Here, on the one hand, silica spheres were formed with an average diameter of $d_{C3N18} = 163 \pm 36$ nm (Figure 1f) with a shoulder to smaller sizes on one side. On the other hand, several micrometer long filament-like structures with a mean diameter of $d_{F\text{-C3N18}} = 33 \pm 17$ nm were visualized. Some of the filaments appeared as a chain of spheres fused together to form tubules (Figure 1f, zoom-in view).

From the SEM images, it was unclear whether the formed silica spheres are solid or hollow in nature. To be able to analyze the interior of the spheres, transmission electron microscopy (TEM) was performed in conjunction with energy dispersive X-ray spectroscopy (EDX). Figure 2 shows TEM bright-field images of silica spheres produced in the presence of C3N6. The spheres appear to be partly solid and partly hollow (Figure 2a,b). However, Figure 2c strongly suggests that the material density is smaller in the interior of the spheres. The thickness of the shells was determined to be 32 ± 2% ($n = 14$) of the diameter of the spheres. To be able to determine the distribution of the compounds from which the silica spheres were made, an EDX analysis was performed. According to Kröger et al.,[8,12] it is expected that SiO_2 and polyamine coprecipitate to form a composite material that is stable even after washing with water. Hence, the precipitate was expected to be composed of four elements, namely, carbon, nitrogen, silicon, and oxygen. Figure 2d shows a scanning TEM (STEM) annular dark-field image of silica spheres produced in the presence of C3N6 with apparently hollow and solid spheres. However, silicon (red) and oxygen (blue), reflecting the position of SiO_2, are restricted only to the shells of the spheres, even in the case where the spheres appear to be solid in the annular dark-field image (see particle 1 in Figure 2d−f). The oxygen signal in line scans and X-ray maps strictly follows the silicon signal with a ratio corresponding to that of SiO_2, showing that there is no significant oxygen signal from any material in the interior of the hollow spheres. The overlay depicted in Figure 2e demonstrates that in addition to silicon (red), carbon (green) is also found in the shells. Spheres that appear solid in the annular dark-field image exhibit an additional carbon signal in their interiors. The small nitrogen signal in the EDX spectra, however, does not significantly exceed the bremsstrahlung background (3σ criterion), so only the carbon content of some hollow spheres can be concluded from the X-ray analyses. These results suggest that the silica spheres are composed of a shell with a thickness of 20−60 nm that consists of SiO_2, while the interior might still contain some polyamine. A similar result was obtained for silica precipitates catalytically formed by C3N12. TEM and STEM images revealed SiO_2 shells with a thickness of 25−50 nm, which is on average 24 ± 4% ($n = 37$) of the sphere diameter (see the Supporting Information). Interestingly, the spheres appear to be hollow in all cases, and the carbon signal in the interior of the spheres is missing. Precipitates induced by the polyamine C3N18 are characterized by two different morphologies. Besides spheres having a SiO_2 shell with a thickness of 20−50 nm [23 ± 3% ($n = 20$) of the spheres' diameter; see the Supporting Information], filamentous structures were found that were also composed of SiO_2, as proven by EDX analysis.

N-Methylation of Polyamines. Long-chain polyamines of diatoms contain nonmethylated as well as methylated amino groups.[14] Recently, for a short-chain C3N3 molecule, it has been demonstrated that the methylation pattern alters the kinetics of the first condensation reaction of silicic acid.[23] Here we chose the long-chain polyamine C3N12, as this compound was proven to precipitate very well defined hollow silica spheres. We methylated all of the secondary amino groups (C3N12Me) and compared the obtained results with those of the nonmethylated molecule. The amount of silica precipitated in the presence of C3N12Me was determined by the β-silicomolybdate method

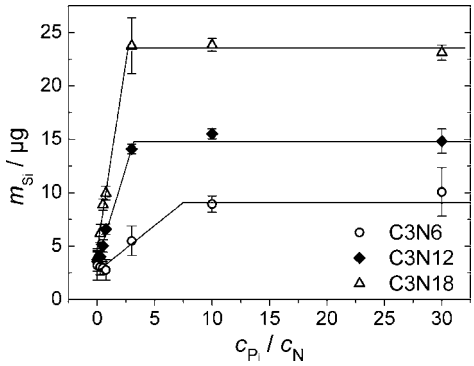

Figure 3. Mass of precipitated silica (m_{Si}) as a function of the phosphate to nitrogen ratio c_{P_i}/c_N for the three different long-chain polyamines C3N6, C3N12, and C3N18. Precipitates were obtained in 30 mM acetate buffer (pH 6.8) with $c_N = 1$ mM and $c_{Si(OH)_4} = 100$ mM. The reaction time was set to 10 min.

to be $m_{Si} = 31.0 \pm 1.5$ µg ($n = 2$), which is a factor of 2 larger than the m_{Si} obtained in the case of C3N12. More interesting was the fact that the SEM images of the precipitates revealed two well-defined populations of silica spheres formed in the presence of C3N12Me (see the Supporting Information). One distribution exhibited an average diameter of $d_{1\text{-C3N12Me}} = 59 \pm 24$ nm, but the majority of spheres had an average diameter of $d_{2\text{-C3N12Me}} = 183 \pm 27$ nm.

Influence of Phosphate Ions on Precipitation. Long-chain polyamines from diatom biosilica are extracted from aqueous solution by chloroform/methanol and thus behave like amphiphilic substances. It is expected that long-chain polyamines in aqueous solutions form aggregates with positively charged surfaces, with the tendency to form larger aggregates in the presence of multivalent anions.[17] To prove this idea, we performed dynamic light scattering (DLS) experiments with C3N6, C3N12, and C3N18 in aqueous solution. The DLS results verified the presence of particles exhibiting hydrodynamic diameters of several hundred nanometers with a rather broad distribution (see the Supporting Information) in the presence of 30 mM phosphate. For C3N12, the influence of the phosphate concentration was further investigated, and it was found that a larger phosphate concentration leads to larger hydrodynamic diameters, i.e., larger droplet sizes (see the Supporting Information). These results support the notion that the polyamines form emulsions of microdroplets in aqueous solution and that droplet formation is a function of the number of multivalent anions. We further investigated the influence of the phosphate concentration on the precipitation products of C3N6, C3N12, and C3N18. Independent of the polyamine, the amount of precipitated silica increased with increasing phosphate concentration (Figure 3) until saturation occurred. Two distinct regions were defined for each plot, a linear one and a constant one. For C3N6, linear behavior of the mass of precipitated silica as a function of the c_{P_i}/c_N ratio with a slope of 0.9 ± 0.5 µg was found. The amount of precipitated silica became independent of the phosphate concentration at a c_{P_i}/c_N ratio of 7.5 with an m_{Si} value of 9.1 ± 0.7 µg. The slope for C3N12, 3.5 ± 0.2 µg, was almost a factor of 4 larger than that of C3N6. At the much smaller c_{P_i}/c_N ratio of 3.2, the precipitation mass became independent of the phosphate concentration in solution and levels off at a value of $m_{Si} = 14.8 \pm 0.7$ µg. In the case of C3N18, the phosphate concentration (i.e., the c_{P_i}/c_N ratio) to precipitate the maximum amount of silica, $m_{Si} = 23.6 \pm 0.7$ µg, was even further reduced to 2.7. The sensitivity of the precipitation reaction with respect to the phosphate concentration, given as the linear increase in m_{Si} as a function of the c_{P_i}/c_N ratio with a value of 7.0 ± 0.8 µg, is further increased by a factor of 2 relative to the slope obtained for C3N12.

For all three compounds, the precipitates obtained at three different phosphate concentrations (3, 10, and 30 mM P_i) were investigated by means of SEM, and the size of the resulting silica spheres was analyzed by histograms. The results are presented in Figure 4. Only a small amount of silica was precipitated with C3N6 (Figure 4a) at 3 mM phosphate. As a result, besides some spherical structures with diameters of $d_{1\text{-C3N6}} = 58 \pm 17$ nm (3 mM P_i) and $d_{2\text{-C3N6}} = 121 \pm 26$ nm (3 mM P_i), some rather nondefined silica structures were also formed. An increase in the phosphate concentration to 10 mM generated more well-defined silica structures; in particular, smooth silica spheres with a mean diameter of $d_{C3N6} = 111 \pm 15$ nm (10 mM P_i) were formed. An even further increase in the phosphate concentration then only slightly increased the average sphere diameter to $d_{C3N6} = 128 \pm 42$ nm (30 mM P_i), with an overall broader size distribution. Interestingly, the influence of the phosphate concentration on the silica morphology was very small in case of C3N12 (Figure 4b). Here, silica spheres having average diameters of very similar sizes were formed, with $d_{C3N12} = 93 \pm 22$ nm (3 mM P_i), $d_{C3N12} = 101 \pm 21$ nm (10 mM P_i), and $d_{C3N12} = 106 \pm 24$ nm (30 mM P_i). This did not hold for the longest polyamine that was investigated in this study, C3N18 (Figure 4c). From the experiments at 30 mM phosphate, we already know that besides silica spheres, filament-like structures with diameters of 30−40 nm were also formed. This was not the case at 3 mM phosphate. Under these conditions, only spheres with a diameter of $d_{C3N18} = 80 \pm 18$ nm (3 mM P_i) were formed. Filament-like structures were, however, formed at 10 mM phosphate. Besides these filaments, two different spherical distributions could be distinguished, with mean diameters of $d_{1\text{-C3N18}} = 25 \pm 7$ nm and $d_{2\text{-C3N18}} = 130 \pm 19$ nm (10 mM P_i). Interestingly, the size of the small spheres was in the same range as the diameter of the filaments and might be interpreted as a prestate of the filaments or vice versa. The same kind of size distribution, but with slightly larger diameters, was found for 30 mM phosphate. Here, filaments were the predominant structures. Average sphere diameters of $d_{1\text{-C3N18}} = 30 \pm 10$ nm and $d_{2\text{-C3N18}} = 154 \pm 46$ nm (10 mM P_i) were measured. In comparison with the result obtained for C3N18 in the presence of 30 mM phosphate (Figure 1f), here two different size distributions were found as a result of the slightly different experimental conditions. However, in principle, the formation of small silica spheres might already be indicated in the shoulder of the histogram in Figure 1f. In summary, the combination of polyamine chain length with propyleneimine units and the phosphate concentration significantly determines the amount and structure of the resulting silica precipitates. However, a correlation between the droplet size found in solution prior to silica precipitation and the resulting structure of the precipitates was not found. Independent of the polyamine, the droplets were considerably larger than the resulting silica particles (see the Supporting Information).

Discussion

To date, no synthetic route has been described for obtaining large quantities of well-defined long-chain polyamines, which are one class of important compounds involved in silica

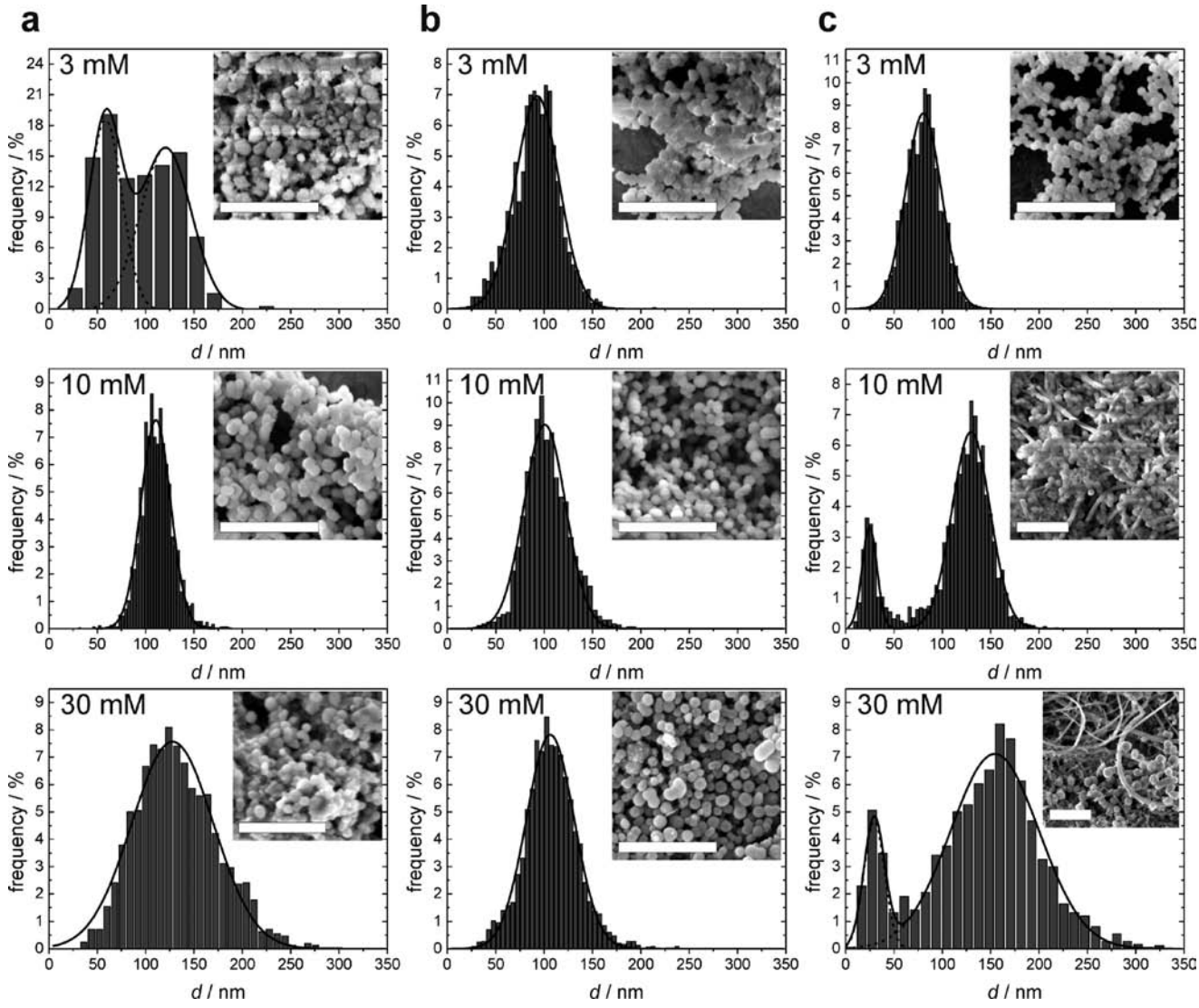

Figure 4. Histogram analyses and corresponding scanning electron micrographs of the silica precipitates obtained in the presence of (a) C3N6, (b) C3N12, and (c) C3N18 using three different phosphate concentrations (3, 10, and 30 mM). Silica precipitates were generated in 30 mM acetate buffer (pH 6.8) with $c_N = 1$ mM and $c_{Si(OH)_4} = 100$ mM. Scale bars are 1 μm.

production in diatoms and sponges. The synthesis of oligoamides on a solid support using well-established peptide synthesis protocols followed by reduction and cleavage of the oligoamines from the resin proved to be superior to the stepwise assembly of oligoamines in solution. Deletion sequences from incomplete couplings of oligoamides are easily identified and can be discarded, while the uniformity of the chain length of oligoamines can be verified by mass spectrometry. The presented protocol avoids the analytical characterization of oligoamines until the final reduction step.

With the well-defined compounds in hand, it was the aim of this study to gain new insights into in vitro silica formation to facilitate the synthesis of distinct silica nanostructures under mild conditions. It was originally recognized by Mizutani et al.[40] that amines and polyamines are capable of accelerating silicic acid polymerization. The group proposed that the polyamine acts as an acid−base catalyst, thus facilitating condensation of two monosilicic acid molecules. Accordingly, the transition state may be stabilized by two appropriately arranged amino groups within the polyamine backbone. Indeed, we found that when the spacer between two adjacent amino groups was composed of only two C atoms, only a very small number of silica spheres were precipitated. Through the use of propyleneimino subunits instead of ethyleneimino subunits, the amount of silica was greatly increased by a factor of ~8. Notably, long-chain polyamines isolated from diatom species have also been characterized as poly(propyleneimime) chains with up to 20 repeat units. Coradin et al.[41] proposed that the protonated amino groups serve as binding sites for silicic acid. The protonation state was calculated, and the charge distribution and hydrophobicity of each polyamine were estimated (see the Supporting Information). The results are summarized in Figure 5 along with the respective precipitated silicon masses. While only 56% of the amino groups are protonated in C2N7, 73% are protonated in the case of C3N7 at pH 6.8, which reflects the greater distance between two amino groups. Separating the amino groups by four C atoms (C4N7) results in protonation

(40) Mizutani, T.; Nagase, H.; Fujiwara, N.; Ogoshi, H. *Bull. Chem. Soc. Jpn.* **1998**, *71*, 2017–2022.

(41) Coradin, T.; Durupthy, O.; Livage, J. *Langmuir* **2002**, *18*, 2331–2336.

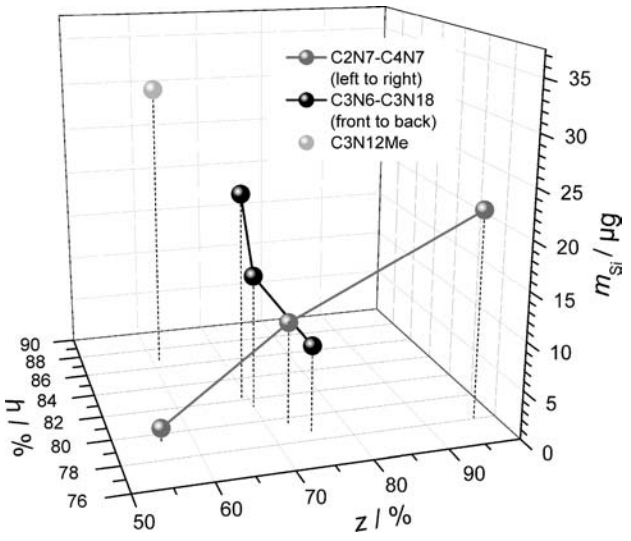

Figure 5. Relationship between the amount of precipitated silica (given as m_{Si}), the protonation state z, and the hydrophobic character h of the polyamines C3N6, C3N12, C3N18, C2N7, C3N7, C4N7, and C3N12Me.

of 97% of the amino groups. However, the hydrophobicity is independent of the N-to-N distance and was estimated to be 78−79%. Figure 5 shows that an almost linear relationship between the relative protonation state and precipitated silica mass is found. One has to keep in mind that the calculation is only a rough approximation, as the formation of emulsions of microdroplets as well as phosphate anions were not taken into account.

It is known that each diatom species exhibits characteristic silica structures on the micro- and mesoscale as well as very specific patterns on the nanoscale,[42] which among other factors is concomitant with the observation that each species is equipped with specific polyamine structures. Structural variations include the overall chain length, the degree of methylation, and the positions of secondary and tertiary amino groups.[43] These findings may imply that the polyamine structures are a determinant for the species-specific nanopatterning of diatom biosilica. Here we found that the structure (i.e., the size of the silica spheres) is significantly increased when the distance between two amino groups is increased, even though the number of nitrogen atoms is constant. This result might reflect the interplay between charge repulsion between ammonium cations and electrostatic attraction with phosphate anions, which results in a particular supramolecular assembly acting as the template for silica precipitation, as proposed by Sumper[16] and discussed below.

When the distance between the amino groups was kept constant at three C atoms, as is found in natural polyamines,[43] but the chain length was increased stepwise to a length that is typically found in diatoms, a mixture of protonated and unprotonated amino groups was found (see the Supporting Information) with rather similar average protonation states of 75% (C3N6), 70% (C3N12), and 69% (C3N18) at pH 6.8. For these three polyamines, the amount of precipitated silica as well as the diameter of the silica spheres is influenced by the chain length, although the differences are less pronounced than those found for the variation of the N-to-N distance. The silica mass increased by a factor of 1.5 with increasing chain length. From C3N6 to C3N18, the hydrophobicity of the molecules increases, while the relative protonation state slightly decreases (Figure 5). This promotes aggregation of the molecules, as hydrophobic attraction counteracts electrostatic repulsion, which influences the amount and size of the silica structures. This may also explain the different c_{P_i}/c_N ratios that are necessary to obtain the maximum amount of precipitated silica, as discussed below in more detail. The change in diameter of the observed silica spheres with increasing chain length was rather small, while drastic changes in the structure from spheres to filaments were observed. Silica fibers have been described in other studies after application of shear stress or electrostatic fields,[44,45] but these were not applied in our experiments. Van Bommel et al.[46] observed silica with a pearl-necklace-like morphology similar to the structures found in Figure 1f when fibrous organogel networks were used as templates for silica deposition. They proposed a surface mechanism according to which silica formation starts at some random points on a fiber, after which silica grows in a spherical manner and later merges into fibers. A transition between spherical and filament-like structures has also been observed in our experiments and might be an indication of the existence of spherical and filamentous C3N18 polyamine aggregates.

A different level of methylation of the amino groups is another structural characteristic of long-chain polyamines found in different diatom species. While polyamines extracted from *Coscinodiscus granii* cell walls do not exhibit any methylation at all, a higher degree of methylation is for example found in polyamines from *Coscinodiscus wailesii.* Polyamines of *Coscinodiscus concinnus* are permethylated.[43,47] These different methylation patterns suggest that methylation per se is not a requirement for silica formation. It has, however, been shown that increased methylation of the amino groups enhances the reaction rate[48] and that the degree of methylation in polyamines affects their ability to promote silica condensation.[49] Hence, it might be conceivable that different methylation patterns can affect the rate of silica formation and therefore play a role in creating species-specific silica nanostructures. Relative to C3N12 (70% protonation), the degree of protonation of C3N12Me is reduced (61%; see the Supporting Information) while the hydrophobicity in turn is increased, which is in line with the trend that increased hydrophobicity leads to larger silica mass (Figure 5). This observation emphasizes the importance of attractive forces between polyamine molecules. Comparing the silica structures produced by the polyamines C3N12 and C3N12Me also demonstrates that by changing only the methylation pattern, a different structure is obtained. While C3N12 produces a well-defined narrow distribution of silica nanospheres (d_{C3N12} = 169 nm), precipitation in the presence of the methylated compound C3N12Me results in two well-defined populations of silica nanospheres with different diameters ($d_{1\text{-}C3N12Me}$ = 59 nm and $d_{2\text{-}C3N12Me}$ = 183 nm).

(42) Hildebrand, M.; York, E.; Kelz, J. I.; Davis, A. K.; Frigeri, L. G.; Allison, D. P.; Doktycz, M. J. *J. Mater. Res.* **2006**, *21*, 2689–2698.
(43) Sumper, M.; Brunner, E. *ChemBioChem* **2008**, *9*, 1187–1194.
(44) Patwardhan, S. V.; Mukherjee, N.; Clarson, S. J. *J. Inorg. Organomet. Polym.* **2001**, *11*, 117–121.
(45) Rodriguez, F.; Glawe, D. D.; Naik, R. R.; Hallinan, K. P.; Stone, M. O. *Biomacromolecules* **2004**, *5*, 261–265.
(46) van Bommel, K. J. C.; Shinkai, S. *Langmuir* **2002**, *18*, 4544–4548.
(47) Sumper, M.; Lehmann, G. *ChemBioChem* **2006**, *7*, 1419–1427.
(48) Robinson, D. B.; Rognlien, J. L.; Bauer, C. A.; Simmons, B. A. *J. Mater. Chem.* **2007**, *17*, 2113–2119.
(49) Menzel, H.; Horstmann, S.; Behrens, P.; Bärnreuther, P.; Krueger, I.; Jahns, M. *Chem. Commun.* **2003**, 2994–2995.

Independent of the exact molecular structure of the long-chain polyamine, these amphiphilic molecules are thought to undergo phase separation in aqueous solution to form an emulsion of microdroplets.[16] By means of DLS, we also found droplets with a size of several hundred nanometers in the aqueous phase in the presence of phosphate. Silica precipitation is supposed to occur at the interface of the polyamine droplets. As silica is produced on a short time scale, i.e. within minutes, it hinders the silicic acid from diffusing deeper into the polyamine droplet, and thus, the interior of the produced silica spheres is expected to be "hollow" instead of solid. Such "hollow" silica shells were indeed unambiguously revealed by the EDX element maps (Figure 2). The silica shells observed here can be discussed in terms of the phase separation model proposed by Sumper.[18] He suggested that a two-dimensional monolayer of polyamine-containing droplets in the silica deposition vesicle guides silica deposition, with polymerization of silica at the surface of the droplets leading to a honeycomb-like framework. The hollow silica shells observed in this study can be rationalized in a similar way. Three-dimensional droplets of polyamines guide the polymerization at the surface of the droplets, resulting in silica spheres.

The phase separation model also suggests that multivalent anions control the silica precipitation process by modulating the polyamine aggregates. It has been shown that the silica sphere size depends on the phosphate concentration in case of polyamines from *Stephanopyxis turris*, which consist of 15−21 *N*-methylpropyleneimine repeating units.[17] We found that for C3N6, 3 mM phosphate is not sufficient to form well-defined silica aggregates, which is probably a result of the small chain length. With an increase in the phosphate concentration, slightly larger silica spheres were obtained. A similar trend was found for C3N12, where a tendency to form larger sphere diameters with increasing phosphate concentration was found. A significant influence of the phosphate concentration was observed for C3N18. Interestingly, for this polyamine, the silica structure changes from spheres to filaments with increasing phosphate concentration, even though the silicon mass is constant. The same was observed when the polyamine chain length was elongated at a constant phosphate concentration of 30 mM.

The intrinsic tendency of polyamines to form aggregates in aqueous solution as a function of chain length is also reflected by the c_{P_i}/c_N ratio necessary to obtain the maximum silica mass that can be precipitated under these conditions. The longer the polyamine, the less phosphate is required for maximum silica precipitation, probably because of enhanced hydrophobicity, a decreased protonation state, and hence increased attractive interactions between the molecules.

Conclusions

The molecular requirements for long-chain polyamines to form well-defined silica precipitates have been elucidated. By means of solid-phase peptide synthesis, it became possible to tailor these molecules and obtain them in large quantities. This is the prerequisite for controlling the growth of an inorganic material such as silicon dioxide on a short time scale and under ambient conditions. We were able to show that formation of hollow silica spheres with a narrow size distribution as well as filaments becomes possible with such well-defined long-chain polyamines, which might be attractive structures for nanotechnological applications.

Acknowledgment. We thank Hans-Jörg Langer for experimental assistance. Financial support by the VW-Stiftung (I/82 042) is gratefully acknowledged.

Supporting Information Available: Experimental details, TEM and STEM micrographs and EDX element maps (Figures S1 and S2), SEM micrographs and histogram analysis for C3N12Me (Figure S3), hydrodynamic diameters of the polyamine droplets (Table S1), space-filling models with charge distributions of polyamines (Figure S4), and the procedure for calculating the polyamine protonation state (Figures S5 and S6). This material is available free of charge via the Internet at http://pubs.acs.org.

JA9061163